NASA/TM—2012-217695

Large Eddy Simulation of a Film Cooling Flow Injected From an Inclined Discrete Cylindrical Hole Into a Crossflow With Zero-Pressure Gradient Turbulent Boundary Layer

Perry L. Johnson
University of Central Florida, Orlando, Florida

Vikram Shyam
Glenn Research Center, Cleveland, Ohio

August 2012

NASA STI Program . . . in Profile

Since its founding, NASA has been dedicated to the advancement of aeronautics and space science. The NASA Scientific and Technical Information (STI) program plays a key part in helping NASA maintain this important role.

The NASA STI Program operates under the auspices of the Agency Chief Information Officer. It collects, organizes, provides for archiving, and disseminates NASA's STI. The NASA STI program provides access to the NASA Aeronautics and Space Database and its public interface, the NASA Technical Reports Server, thus providing one of the largest collections of aeronautical and space science STI in the world. Results are published in both non-NASA channels and by NASA in the NASA STI Report Series, which includes the following report types:

- TECHNICAL PUBLICATION. Reports of completed research or a major significant phase of research that present the results of NASA programs and include extensive data or theoretical analysis. Includes compilations of significant scientific and technical data and information deemed to be of continuing reference value. NASA counterpart of peer-reviewed formal professional papers but has less stringent limitations on manuscript length and extent of graphic presentations.

- TECHNICAL MEMORANDUM. Scientific and technical findings that are preliminary or of specialized interest, e.g., quick release reports, working papers, and bibliographies that contain minimal annotation. Does not contain extensive analysis.

- CONTRACTOR REPORT. Scientific and technical findings by NASA-sponsored contractors and grantees.

- CONFERENCE PUBLICATION. Collected papers from scientific and technical conferences, symposia, seminars, or other meetings sponsored or cosponsored by NASA.

- SPECIAL PUBLICATION. Scientific, technical, or historical information from NASA programs, projects, and missions, often concerned with subjects having substantial public interest.

- TECHNICAL TRANSLATION. English-language translations of foreign scientific and technical material pertinent to NASA's mission.

Specialized services also include creating custom thesauri, building customized databases, organizing and publishing research results.

For more information about the NASA STI program, see the following:

- Access the NASA STI program home page at *http://www.sti.nasa.gov*

- E-mail your question to *help@sti.nasa.gov*

- Fax your question to the NASA STI Information Desk at 443–757–5803

- Phone the NASA STI Information Desk at 443–757–5802

- Write to:
  STI Information Desk
  NASA Center for AeroSpace Information
  7115 Standard Drive
  Hanover, MD 21076–1320

NASA/TM—2012-217695

Large Eddy Simulation of a Film Cooling Flow Injected From an Inclined Discrete Cylindrical Hole Into a Crossflow With Zero-Pressure Gradient Turbulent Boundary Layer

Perry L. Johnson
University of Central Florida, Orlando, Florida

Vikram Shyam
Glenn Research Center, Cleveland, Ohio

Prepared under Contract NNC097A01C

National Aeronautics and
Space Administration

Glenn Research Center
Cleveland, Ohio 44135

August 2012

Acknowledgments

The author is grateful for the mentoring support of Dr. Vikram Shyam through the Lewis Educational Research Collaborative Internship Program (LERCIP) with the Ohio Aerospace Institute (OAI). The author benefited from helpful discussions with Drs. Shyam, Lamyaa El-Gabry, and Ali Ameri concerning the experimental data and numerical techniques.

This work was sponsored by the Fundamental Aeronautics Program at the NASA Glenn Research Center.

Level of Review: This material has been technically reviewed by technical management.

Available from

NASA Center for Aerospace Information
7115 Standard Drive
Hanover, MD 21076–1320

National Technical Information Service
5301 Shawnee Road
Alexandria, VA 22312

Available electronically at http://www.sti.nasa.gov

Large Eddy Simulation of a Film Cooling Flow Injected From an Inclined Discrete Cylindrical Hole Into a Crossflow With Zero-Pressure Gradient Turbulent Boundary Layer

Perry L. Johnson
University of Central Florida
Orlando, Florida 32816

Vikram Shyam
National Aeronautics and Space Administration
Glenn Research Center
Cleveland, Ohio 44135

Abstract

A Large Eddy Simulation (LES) is performed of a high blowing ratio (M = 1.7) film cooling flow with density ratio of unity. Mean results are compared with experimental data to show the degree of fidelity achieved in the simulation. While the trends in the LES prediction are a noticeable improvement over Reynolds-Averaged Navier-Stokes (RANS) predictions, there is still a lack a spreading on the underside of the lifted jet. This is likely due to the inability of the LES to capture the full range of influential eddies on the underside of the jet due to their smaller structure. The unsteady structures in the turbulent coolant jet are also explored and related to turbulent mixing characteristics.

Introduction

It is well known that film cooling is one of the useful techniques that help the metal components survive in the extremely harsh environment immediately downstream of the combustion chamber of a gas turbine. With improvement of film cooling design, this combustion temperature continues to increase over time. Higher temperatures of the combustion products yield higher efficiencies for the turbine. For film cooling, compressed air is drawn from the compressor stage and injected through film holes, which are machined in the metal surface of the blades and endwalls. These coolant jets then create a blanket-like effect to protect the solid surface from the hot main flow. Although the film cooling technique has been successfully implemented in the gas turbine industry, it is still in the process of both improvement and optimization. The designer always wants to achieve the best capability to protect the surface from the high mainstream temperature using least amount of coolant in order to achieve higher gas turbine cycle efficiency.

The simplest discrete hole film cooling geometry is the cylindrical hole (Goldstein et al. 1968, Goldstein et al. 1970, Eriksen et al. 1974), which is typically inclined at an angle around 30° to 35° to the crossflow. The dominance of the detrimental counter-rotating vortex pair leads to diminished effectiveness on the downstream wall (Haven et al. 1997). While the streamwise cylindrical hole is the simplest film hole configuration, many alternate geometries have been shown to provide better effectiveness downstream of the hole. The most notable of these variations include: compound angle holes (Ligrani et al. 1994a-b, Sen et al. 1996, Schmidt et al. 1996), diffusion-shaped holes (Bunker 2005), and trenched holes (Bunker 2001, Bunker 2002).

The focus of the present paper is to study the unsteady interactions of a compound angle film cooling hole using LES. Film cooling scenarios have typically been studied using the Reynolds-Averaged Navier-Stokes equations (RANS) with two-equation turbulence models (Walters and Leylek 2000, McGovern and Leylek 2000, Hyams and Leylek 2000, Brittingham and Leylek 2000). In particular, latter two study the time-averaged flow features of compound angle holes using the RANS numerical approach. RANS analysis is a steady flow approach, which yields time-averaged results by using various viscous models to account for the effects of turbulence. LES, however, directly resolves the more influential turbulent scales by solving

the Navier-Stokes equations in both the spatial and temporal domains. In this way, LES captures the effects of the problem-dependent, high energy large scale velocity fluctuations in the studied flow field. Acharya et al. (2001) studied LES predictions of square hole geometries and concluded that the two equation turbulence models, used with the RANS equations, overpredict the vertical penetration and underpredict the lateral spreading of the coolant jet. They showed that LES solutions predicted mean velocities and turbulent stresses better than RANS models. Furthermore, Tyagi and Acharya (2003) used LES to study cylindrical inclined coolant holes more closely. Not only did LES enable them to identify the known vortical structures of a jet in crossflow (Fric and Roshko 1994, Kelso et al. 1996, Haven and Kurosaka 1997), but also led them to propose a unifying 'hairpin' vortex structure. They concluded that their LES results matched previous experimental results of Lavrich and Chiappetta (1990) and Sinha et al. (1991) with few discrepancies. Ultimately, they suggested that their observations of the LES solution showed a high significance of the shortcomings of the RANS models.

More recent film cooling LES studies were performed by: Iourokina and Lele (2006a-b), Peet and Lele (2008), Leedom and Acharya (2008), Guo et al. (2006), and Renze et al. (2008a-c, 2009). The present study simulates a cylindrical film cooling hole with high blowing ratio than typically simulated, specifically, M = 1.7. This high of a blowing ratio, while not ideal, can still play a role in engine performance during aircraft cruise, since film cooling is typically designed to survive the tougher conditions at take-off.

Numerical Methodology

The open source software OpenFOAM was used for solving the filtered governing equations for mass, momentum, and energy conservation. OpenFOAM uses the finite volume method (FVM) of discretization on unstructured grids.

Experimental Data for Validation

Data from the experiments of El-Gabry (2011) for film cooling flow fields is used for validation of mean and second-order statistics. The numerical domain and boundary conditions are constructed so as to best approximate the experimental conditions.

Main Simulation

Domain and Boundary Conditions

The numerical domain (Fig. 1) included one full pitch with one cooling hole in the center and periodic planes on either side. The surface boundary was an adiabatic wall satisfying the no-slip conditions. The grid was clustered near the wall such that the viscous sublayer was satisfactorily resolved ($y+ <1$). The height of the solution domain was 5 diameters, as suggested by Johnson et al. (2010). At the free-stream boundary, the streamwise velocity was specified and the other two velocity components were given zero gradients. All other variables were specified with zero gradients. The domain for the main simulation was chosen to include enough space upstream of the hole for the inclusion of the recycling technique to be merged with the main solution, which provided the velocity inlet conditions. Specifically, the domain extended 12 diameters upstream of the injection, with the recycling plane ~5.5 diameters upstream of injection and ~6.5 diameters (~70 displacement thicknesses) downstream of the inlet plane. In this way, no auxiliary simulation was needed in parallel with the main simulation (only for initialization of the main solution). A constant temperature was specified at the cross-flow inlet. Downstream, the domain was extended 12 diameters downstream of the injection, far enough for comparison with relevant experimental data but not too far as to reach a point where the merging of the jets completely invalidates the physics of the periodic boundary conditions. The advective boundary condition using local fluid velocity was specified on the outflow plane.

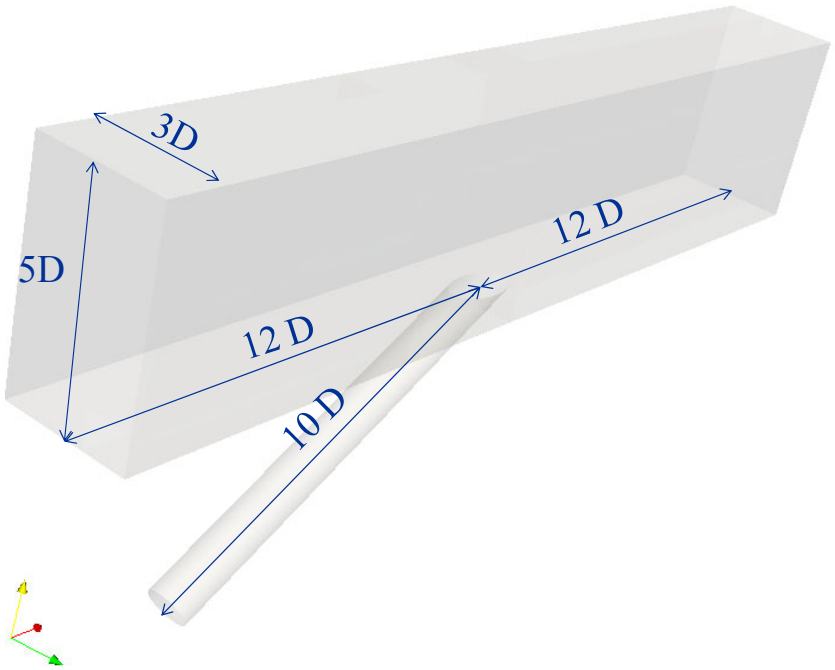

Figure 1.—Extent of numerical domain.

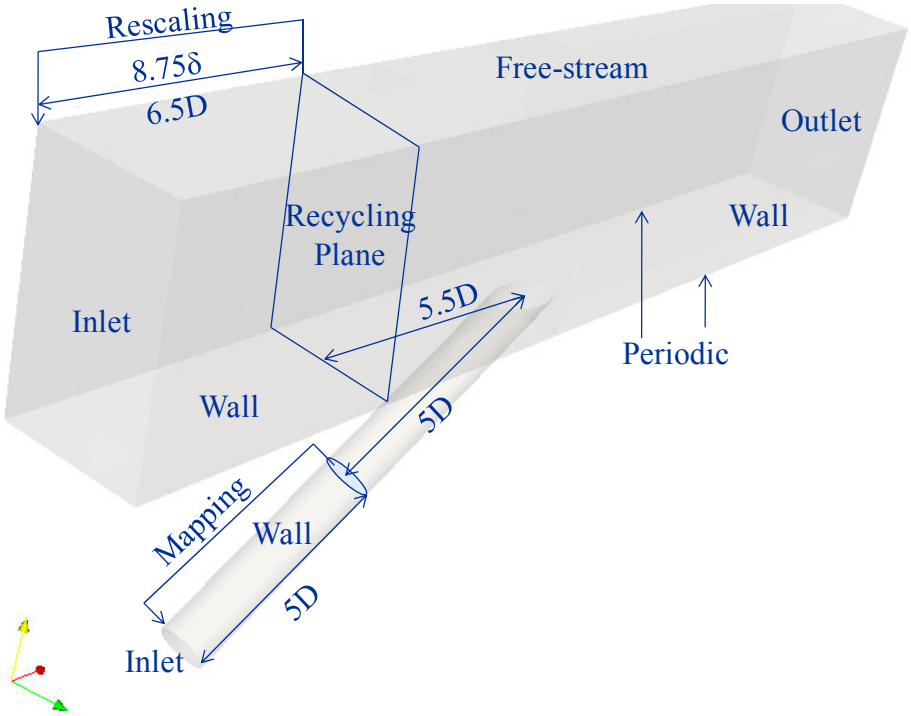

Figure 2.—Boundaries for full numerical domain.

No coolant plenum was modeled and the coolant hole was supplied with “fully-developed” turbulent pipe flow, so as to best match experimental conditions in a time-resolved manner. The cylindrical coolant hole was an adiabatic, no-slip wall. The different boundaries are shown in Figure 2. The specifics of the boundary conditions are summarized in Table 1.

TABLE 1.—BOUNDARY CONDITIONS FOR FULL NUMERICAL DOMAIN

Boundary	Velocity	Pressure	Temperature	Other
Inlet	recycled(crossflow rescaled)	Zero-gradient	297 K	Zero-gradient
Wall	$U_x=U_y=U_z=0$ m/s	Zero-gradient	Adiabatic	Zero
Free-stream	$U_x=U_\infty$, U_y,U_z: zero-gradient	$p = p_\infty$	Zero-gradient	Zero-gradient
Outlet	Advective	Zero-gradient	Zero-gradient	Zero-gradient

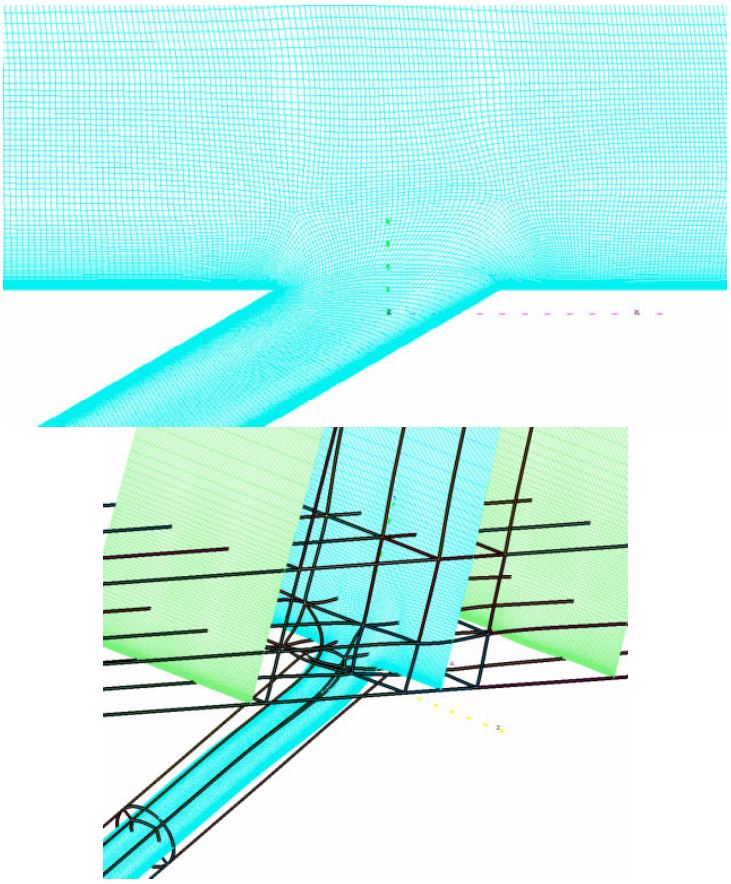

Figure 3.—Computational grid.

Grid and Spatial Discretization

The domain was discretized using the finite volume method in OpenFOAM. The numerical grids were generated using the GridPro software available commercially from Product Development Company (PDC). The grids were generated in a block-structured manner but converted to unstructured format for use with OpenFOAM. The final grid consisted of about 9 million hexahedral cells. Near the no-slip walls, the grid was refined such that the first cell fell within $y+ < 1$. For the boundary layer simulation, the streamwise spacing was $x+ \sim 35$, and the spanwise spacing was $z+ \sim 16$. These spacings were continued throughout the domain with the ratio of the boundary layer thickness to coolant hole diameter being ~0.75. The main simulation grid is shown in Figure 3.

All diffusive Laplacian terms were discretized using a second-order centered scheme, consistent with the nature of diffusion. The convective terms were likewise discretized with second-order central schemes, but limiters were introduced to maintain solution stability and boundedness.

Solution Technique and Temporal Discretization

The incompressible Navier-Stokes equations were solved along with the continuity and energy equations. A low-pass filtering operation in three-dimensional space was implicitly performed by the grid. Residual stresses not resolved by the grid were modeled using the dynamic procedure of Germano (1991), specifically with the modification of Lilly (1992). The solution was progressed in time such that the Courant number was kept well below 0.5 in regions of high interest. This allowed for the time-accurate resolution of the non-filtered scales. The second-order fully-implicit backwards-differencing method was used to discretize all temporal derivatives. A PISO-SIMPLE scheme was used for time advancement. The SIMPLE iteration technique was used to converge the solution at each time step, with multiple pressure corrections in each SIMPLE iteration (resembling the PISO method). Typical time steps employed three SIMPLE ("outer") iterations and two pressure corrections ("inner iterations"). The initial conditions for the simulation were developed by converging the full domain using a steady solver (SIMPLE) with the RANS equations and k-ω SST turbulence model. Then, the results of two precursor simulations were mapped onto the domain and the simulation was started.

Precursor Simulations

In order to hasten the development of a fully turbulent boundary layer within the recycling domain upstream of the film injection, the boundary layer simulation was started on a considerably smaller domain. The goal was merely to initialize the corresponding portion of the full simulations with a realistic turbulent boundary layer. Similarly, the upstream portion within the coolant tube was also developed first in a preliminary simulation before used to initialize the instantaneous velocities as fully developed pipe flow. The numerical grids for these precursor simulations were extracted from the numerical grid from the full simulation such that there was direct mapping to transfer the results of the precursor simulation to the initialized full simulation.

Similarly, the first five diameters of the coolant pipe was extracted from the grid and simulated separately. This also was mapped directly onto the simulation initialized flow field.

Domain and Boundary Conditions

The extent of the boundary layer was 10 disturbance thicknesses in length (~7.5 diameters), 2.67 boundary layer thicknesses normal to the wall (~2 diameters), and the full 3 diameters in the lateral direction with periodic boundary conditions. The grid corresponding to this region upstream of the hole was extracted from the full grid. Figure 4 shows the region extracted from the full domain.

The inlet to the precursor domain followed the specification detailed in Appendix A for generating an inflowing spatially developing turbulent boundary layer. The recycle plane was placed 8.75 disturbance thicknesses (~70 displacement thicknesses) downstream of the inlet to avoid spurious accumulation of error, false periodicity, and unwanted interaction of streamwise-oriented coherent structures (see Jewkes et al. 2011).

The boundary conditions for the sub-domains were specified to reflect the boundary conditions of the main solution as closely as possible. The boundary layer precursor domain inlet, wall and periodic conditions remained identical to the full domain. The free-stream boundary conditions were the same, but moved closer to the wall to reduce the computational cost of the precursor simulation. The outflow, likewise, was an advective outflow condition, as in the main simulation, but was moved necessarily to accommodate the boundary layer simulation. An advective outflow was added to the pipe flow domain, as necessary to close the domain. All other boundary conditions remained identical to the full simulation for the pipe flow precursor.

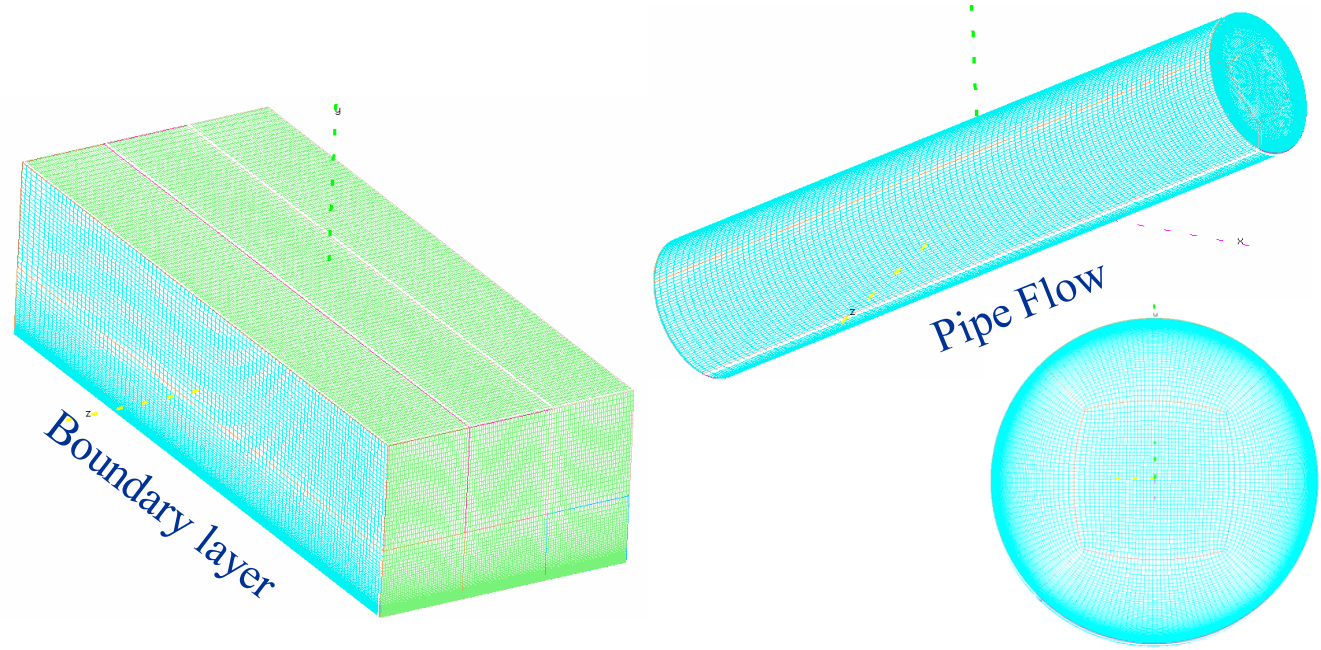

Figure 4.—Two precursor simulation grid extracted from full domain grid.

Grid and Spatial Discretization

As previously mentioned, the grid was created for the precursor simulation simply by extracting the relevant domain from the full solution domain grid. Spatial discretization was the same as applied in the main simulation.

Solution Technique and Temporal Discretization

The solution method was similar to the full simulation. Some differences were applied due to the fact that the grid was very well-behaved compared to some regions of the main simulation near the lip of the coolant hole. The PISO method was applied with no outer iterations at each time step. Three pressure corrections were used within the PISO method to converge the solution at each time step. The semi-implicit Crank-Nicholson scheme was used for temporal discretization precursor simulations. Note that the backward scheme in time was used for the main simulation, due to stability concerns. The simple boundary layer and pipe flow simulations had no such stability problems.

Initialization and Precursor Results

The initial conditions for these simulations are discussed in Appendix B. Figure 5 shows the velocity magnitude at the initialized conditions. The results of the precursor simulations are subsequently shown in Figure 6. The difference is visually perceptible, with the second figure having obtain realistic turbulent structure, whereas the initialization is simply a superposition of random perturbations.

These two results are then mapped onto the full domain simulation, after it has been initialized by converging the RANS equations with k-ω SST turbulent model. Figure 7 shows the final initialized full domain.

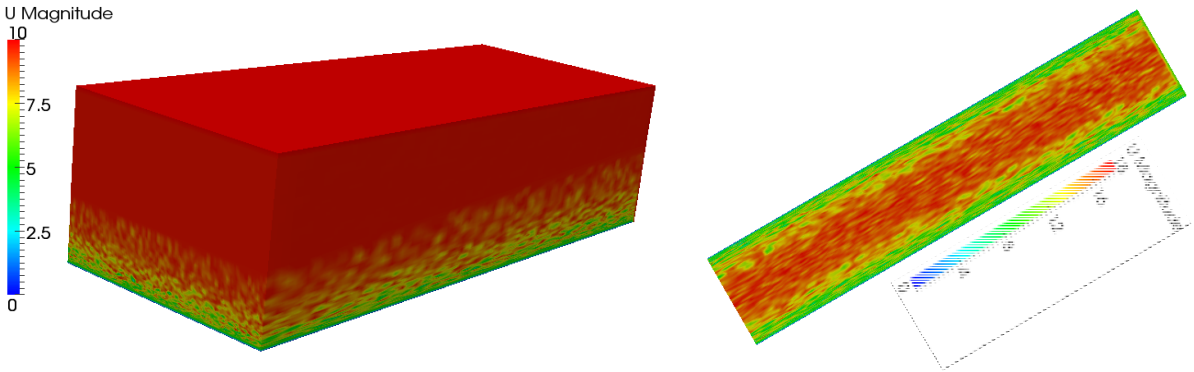

Figure 5.—Initial velocity magnitude contours for precursor simulations (see Appendix B).

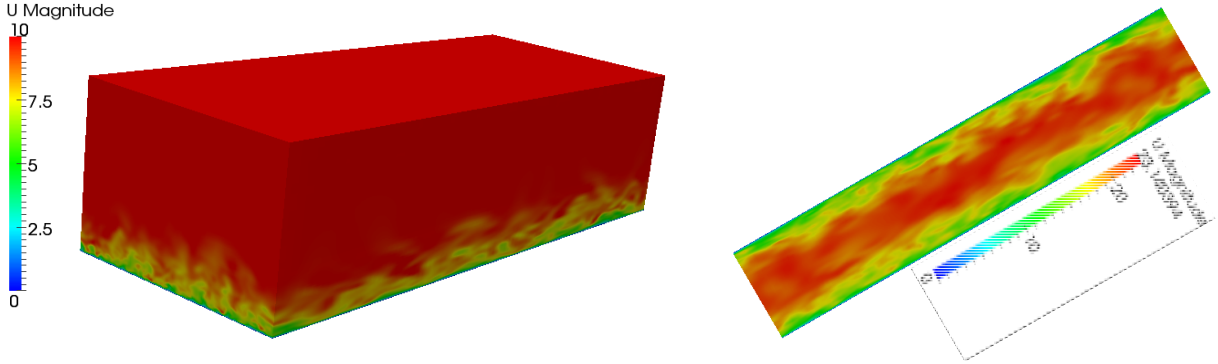

Figure 6.—Final velocity magnitude contours for precursor simulations.

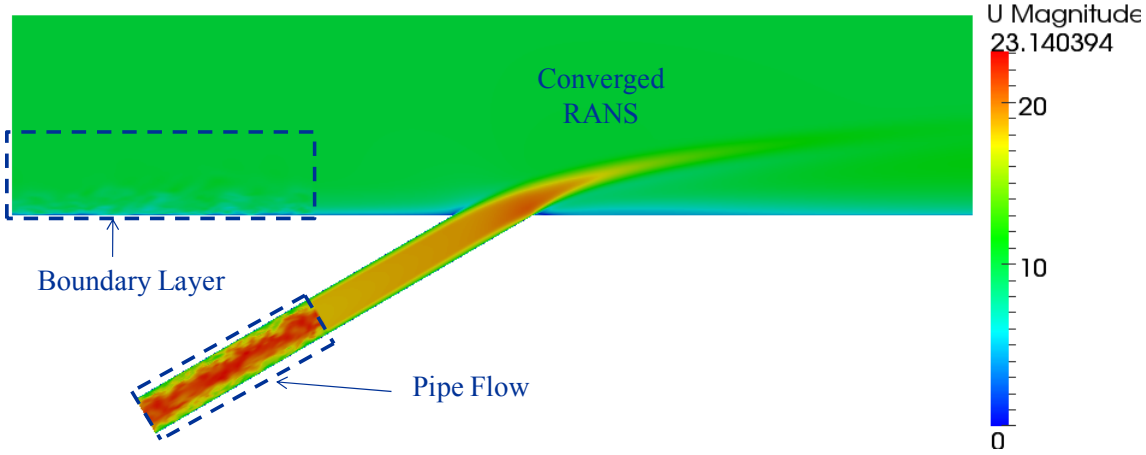

Figure 7.—Initialized velocity for the full domain, with two piecewise mappings superposed on a converged RANS solution.

Results

The simulation was advanced with a time step of 5e-6 sec (~0.0025 D/U_∞). From the initial conditions, the simulation was run for 0.175 sec (~90 D/U_∞) before beginning statistical sampling. Statistical samples were taken over a period of 0.3 sec (~150 D/U_∞).

Mean Profiles

The evolution of the jet is shown in Figures 8 to 12 by non-dimensional temperature contour plots at constant x locations. Comparison with experimental data and RANS solution is shown at each location. The temperature contours best mark the presence of the cooling jet and are of highest interest in the film cooling scenario, since the goal is to provide thermal protection to the adiabatic surface. The streamwise locations are designated by distance downstream of the leading edge of the film hole.

Figure 8 shows the temperature contours at x/d = 2. This is the streamwise location of the trailing edge of the hole. For this reason, the core of the jet remains intact and has only just begun to spread. The experimental results show slightly more initial spreading than either of the numerical results. Most notable is the proximity of the outer part of the coolant to the wall. The experiment shows that the coolant is much closer to the wall.

At x/d = 3, Figure 9, the coolant shows noticeable lift-off behavior. The coolant core is also bent into an upside-down "U-shape". This indicates the presence of a strong counter-rotating vortex in the wake of the jet. The numerical simulations still underpredict the mixing of the coolant, as the coolant core seems to remain more intact than in the experiment. Concerning trajectory, the main difference again is the proximity of the under-side of the jet to the surface. The trajectory of the upper-half of the jet is accurately predicted. Both RANS and LES predictions have trouble matching the experimental data at this point.

The LES begins to show better predictions with the experimental data at the jet progresses to x/d = 4, Figure 10. Certainly, the LES predictions are better than that of the RANS model, which continues is under-prediction of jet's mixing. The LES predicts a more defined upside-down "U" shape than the experiment and still does not show enough spreading back to the wall. Otherwise, the contours are largely in agreement with the experimental data.

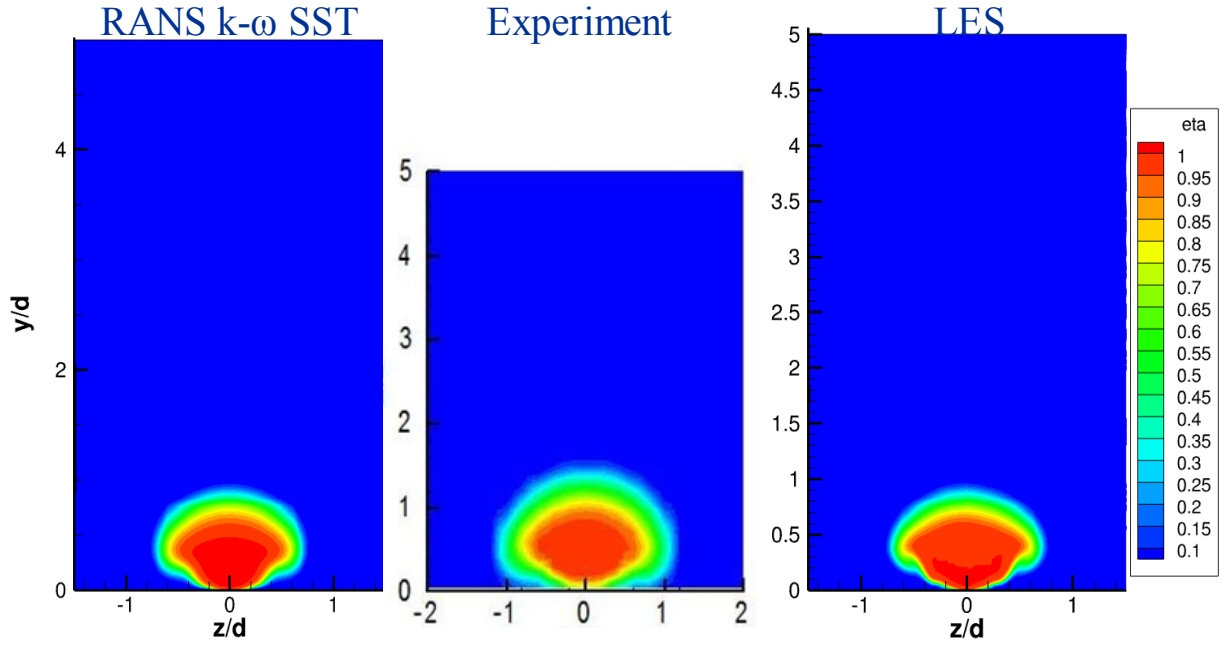

Figure 8.—Comparison of mean non-dimensional temperature contours at x/d = 2 (from the leading edge of the injection).

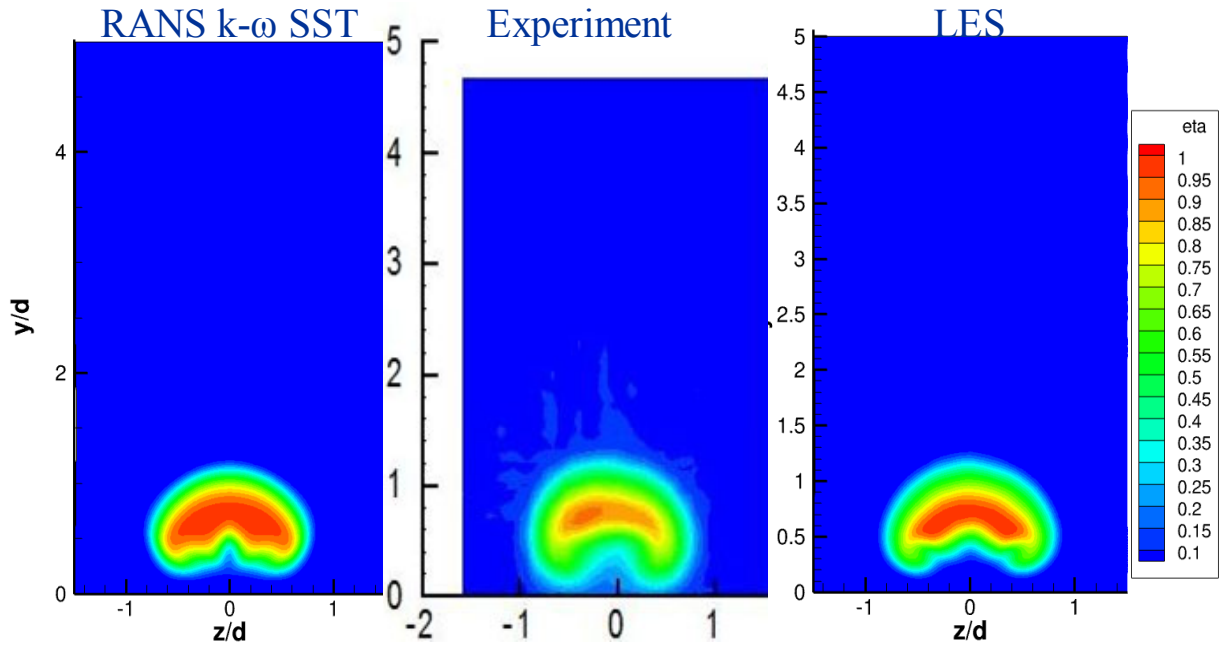

Figure 9.—Comparison of mean non-dimensional temperature contours at x/d = 3.

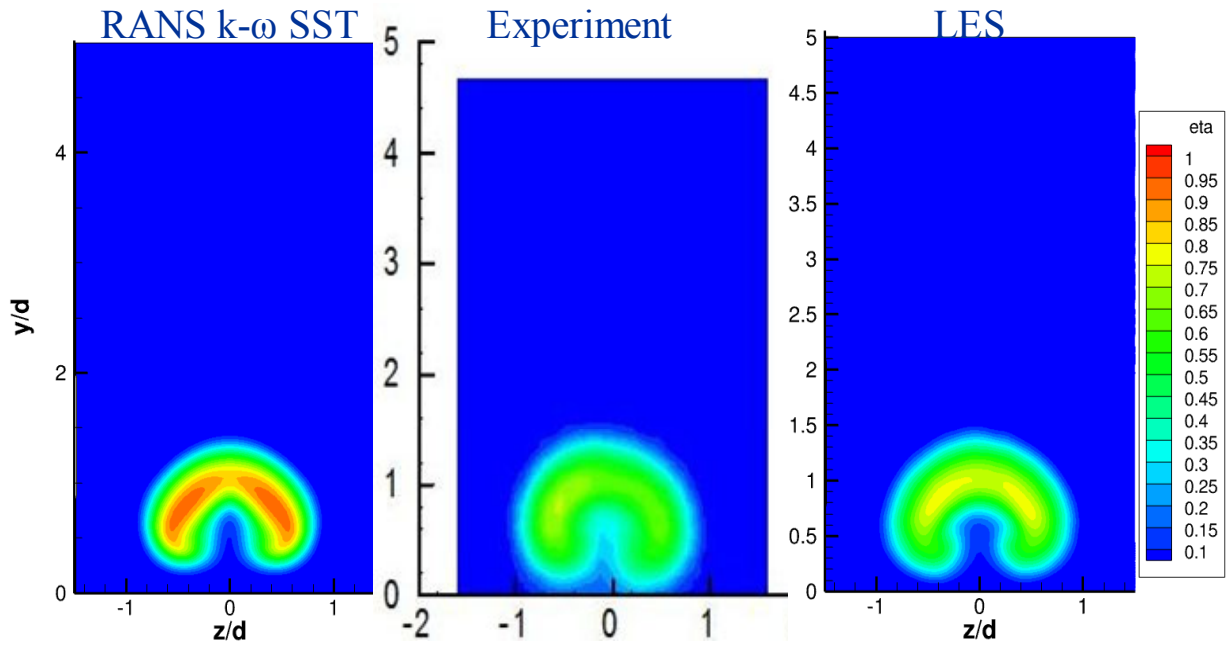

Figure 10.—Comparison of mean non-dimensional temperature contours at x/d = 4.

At x/d = 6, the LES continues to show dramatically better agreement with experiment than the RANS model, Figure 11. The LES shows a slight general under-prediction of spreading in all directions, but this is still most notable on the underside of the jet. The "U" shape of the jet is now mostly blurred by the increased turbulent mixing within the jet and wake regions. The core region of the jet shows temperatures mid-way between those of the coolant and crossflow.

The final streamwise station to be shown is x/d = 8, Figure 12. At this point, it is seen from the experiment that neighboring jets have begun to interact. This places the periodic boundary conditions of the LES in suspect, due to the possibility of enforcing unphysical periodicity. The temperature contours from the experiment show that the spreading of the jet has greatly increases since x/d = 6. The jump in spreading is not mirrored in the LES, though the general shape and position of the jet is well predicted. The RANS model clearly fails to predict the experiment, even qualitatively. The failure of the LES to keep pace with the experiment in the spreading of the jet is attributable to the spanwise boundary conditions. At this location, the adjacent jets have begun to merge and periodic boundary conditions enforce a false periodicity in the time-accurate sense. The experiment consisted of a row of just three film cooling jets, while the current simulation attempts to model an infinite row of jets. Therefore, once the effects of neighboring jets begin to play a noticeable role, the fidelity of the spanwise boundary conditions in matching the experiment is highly questionable.

In all of the streamwise-normal planes, an over-prediction of temperature at the wall is evident. This seems to be caused by the LES model failing to spread back toward the wall at a rate equal to the experiment. A possible explanation is the near wall treatment of the LES. Near solid boundaries, the range of turbulent length scales is shortened due to proximity to impermeability. This puts the theory behind LES on weak grounds. Many attempts, such as DES and two-layer zonal methods, have been made to get around the deficiency of LES near a wall, but all are still under development. No clear solution to the LES near-wall problem has emerged, other than essentially running DNS in the near-wall region. The failure of the current model to resolve enough "large eddies" in the near-wall region is very likely the cause of its failure to properly predict spreading back toward the wall. Since the 'large eddies' in the near-wall region are much smaller than elsewhere in the flow, even with the resolution in the wall-normal direction, the other two dimensions could be filtering out eddies of size and influence crucial to the turbulent mixing in this region. The anisotropy, meanwhile could be preventing the dynamic Smagorinsky model (based on the cube root of the cell volume), from accurately predicting the unresolved turbulent stresses.

Figure 13 shows the temperature contours along the center-plane of the jet. The main difference is again on the underside of the jet, where the temperature is over-predicted (under-prediction in effectiveness). The turbulent mixing is evidently not as strong compared to the lifting force of the counter-rotating vortices in the LES model as compared with experiment. Similarly, x-velocity contours are shown in Figure 14. The maximum velocity in the jet core near the exit of the hole is noticeably different between the LES and the experiment. This points to the experiment's failure to adhere to the nominal conditions, hence a mismatch in blowing ratio between the LES and experiment. Also, the boundary layer is seen to be much thicker in the LES than in the experiment. Other evidence not shown indicates that the recycling boundary layer method upstream of the hole was thickened beyond the desired thickness due to the presence of the hole and this effect was recycled to the inlet. This is clearly undesirable, as a thicker boundary layer would provide less downward forcing on the jet.

In theory, these two mismatches between experiment and simulation have opposite effects. The lower jet velocity in the LES would tend to give it less lift-off and a lower trajectory. Meanwhile, the thicker boundary layer would raise the "effective blowing ratio". The plots shown so far indicate that the mean trajectory was accurately predicted by the LES, indicating that these two effects approximately canceled. The effect of these two considerations on the mixing and spreading of the jet is less certain and an additional consideration when interpreting the differences between experiment and simulation.

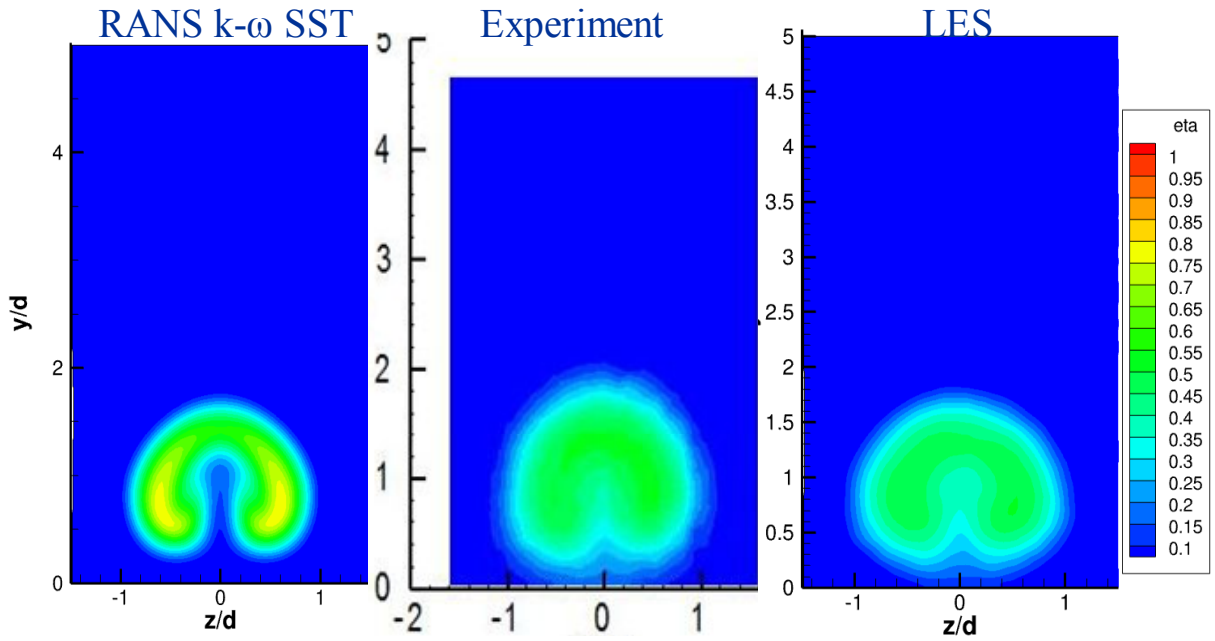

Figure 11.—Comparison of mean non-dimensional temperature contours at x/d = 6.

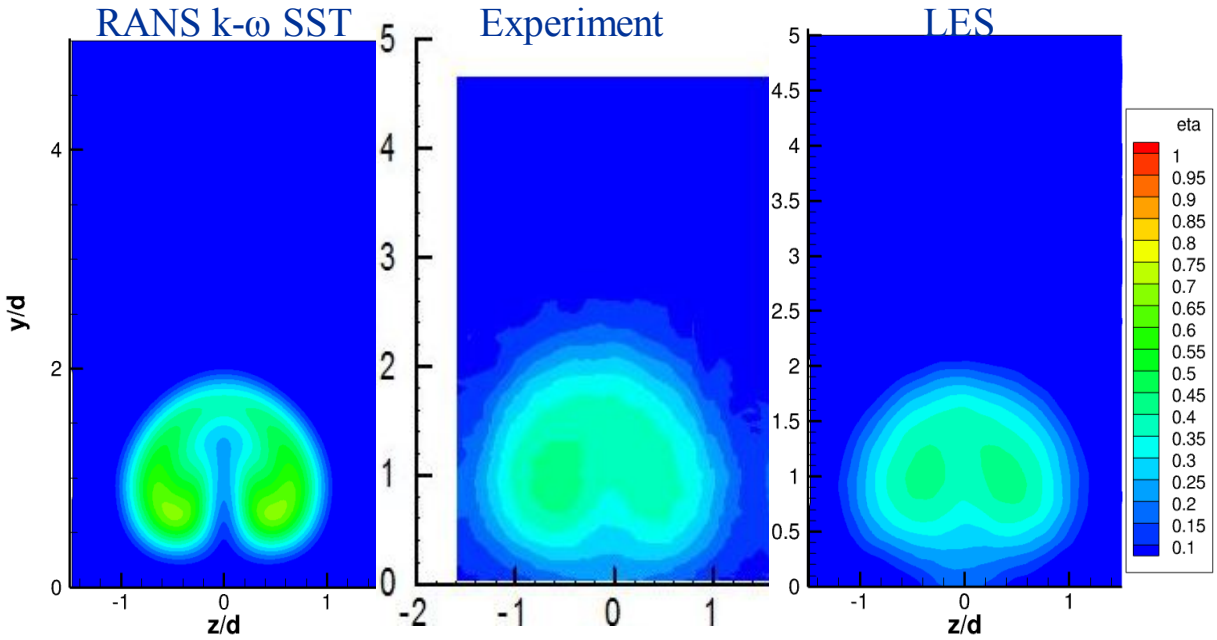

Figure 12.—Comparison of mean non-dimensional temperature contours at x/d = 8.

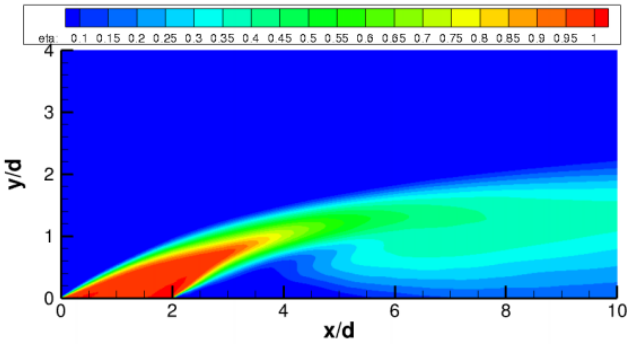

(a)

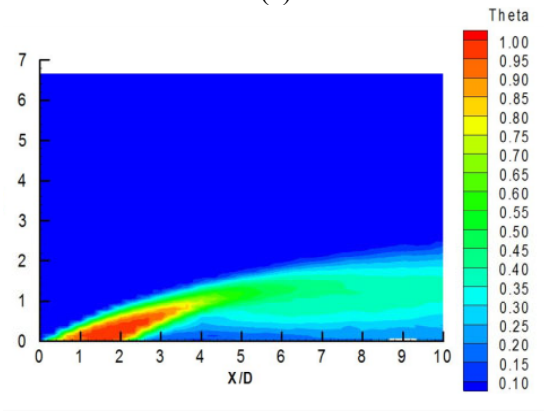

(b)

Figure 13.—(a) LES and (b) experimental centerline mean temperature contours.

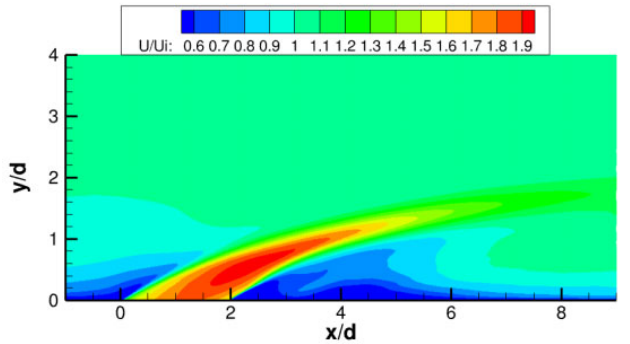

(a)

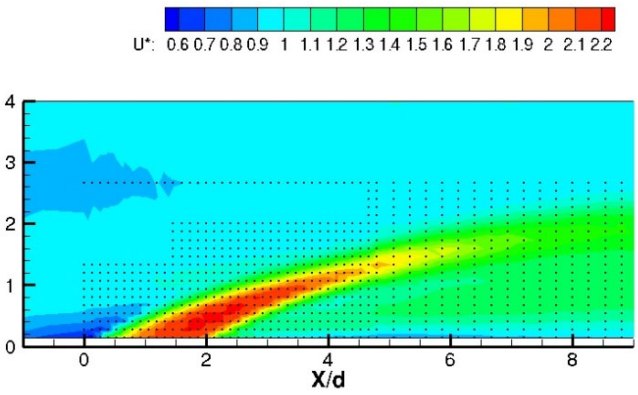

Figure 14.—(a) LES and (b) experimental centerline x-velocity contours.

Unsteady Dynamics

One of the main advantages of the LES approach to simulation over RANS models in the ability to look into the dynamics of the large scale turbulence. Such eddies and structures carry the most influence over the mean statistics, and hence give insight into the cause behind flow features.

Figure 15 shows iso-surfaces of temperature at a time in the flow from different viewing angles. The upper right shows an isometric view, revealing that the breakdown of the jet into unsteady shear layer roller vortices does not happen immediately at the exit of the hole, but after a little while of interaction between the jet and crossflow. This is echoed in the other two views. The upper right view, from the side of the jet, shows the general detached nature of the temperature contours (hence effectiveness) of the coolant. While the coolant appears to spread rapidly in the upper half of the jet, the spreading back toward the surface is subdued. No large structures (from a temperature point of view) are seen in the lower edge of the jet. This reflects that the eddy length scales are damped near the wall and spreading is reduced. The bottom image in Figure 15, looking down on the jet from above, shows the spanwise spreading. The spreading seems to be hindered once the jet starts reaching the edge of the domain, despite the periodic boundary. The hypothesis from above, invoking a false-periodicity in the spanwise direction, could be cited for this phenomenon and the under-prediction of spreading in this region. Shear layer roller vortices, caused by the interaction of the jet with the slower crossflow, are evident on the top and sides of the jet. The presence of an impermeable wall limits their presence on the underside of the jet. These structures are likely liable for the spreading rate of the jet.

Another phenomenon uncovered in the instantaneous results is the occurrences of unsteady reattachment events on the side regions of the jet. Such an event is shown via temperature and shear stress contours at the wall, Figure 16. Figure 17 shows iso-surfaces of temperature from a view underneath the jet at the same time. It is seen that a structure of lower temperature, protruding from the jet, has made significant contact with the surface.

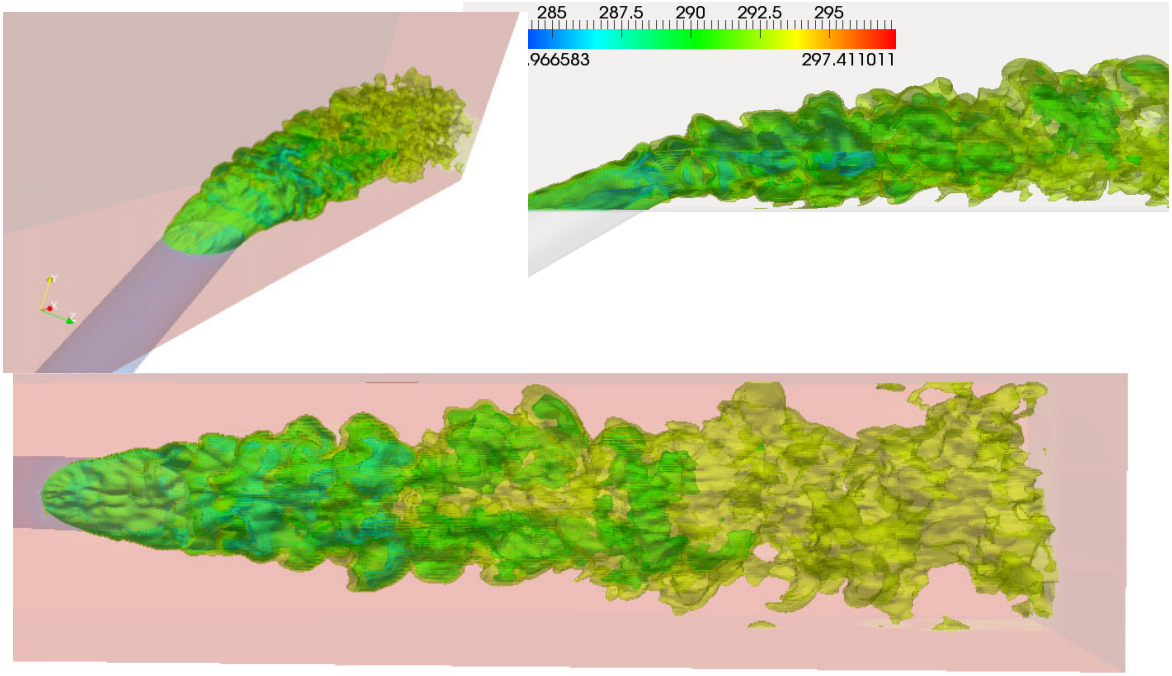

Figure 15.—Iso-surfaces of temperature for the spreading jet.

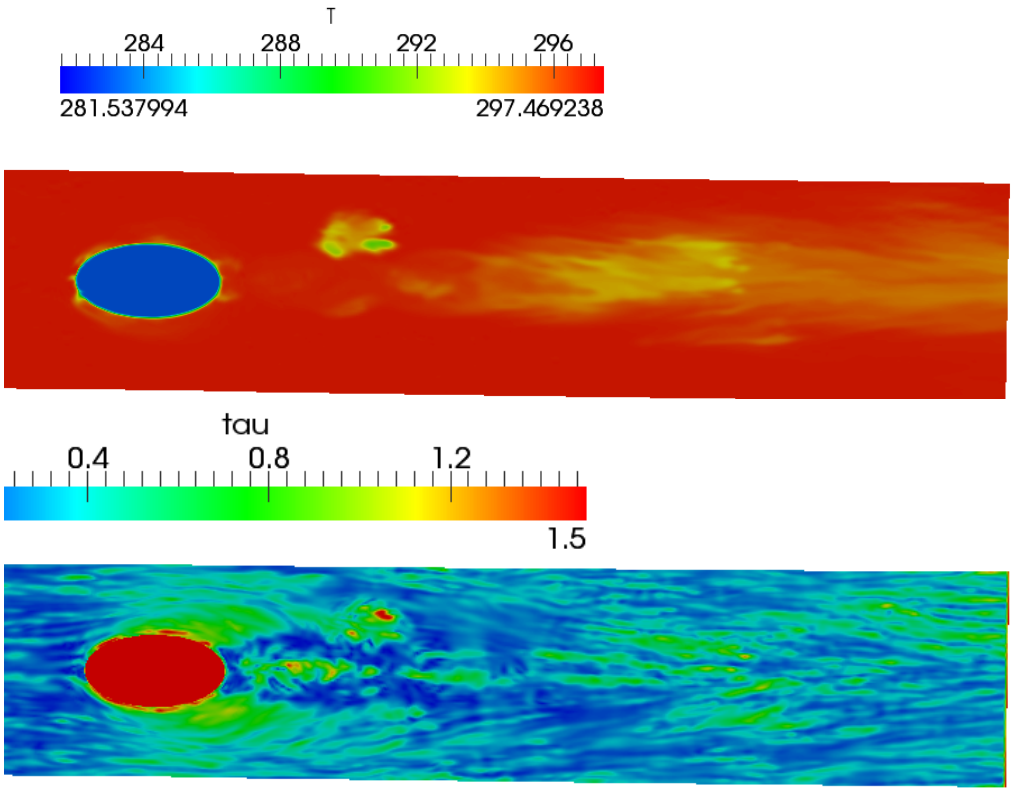

Figure 16.—Contours of temperature and skin friction on the adiabatic surface, showing a re-attachment event on the side of the jet.

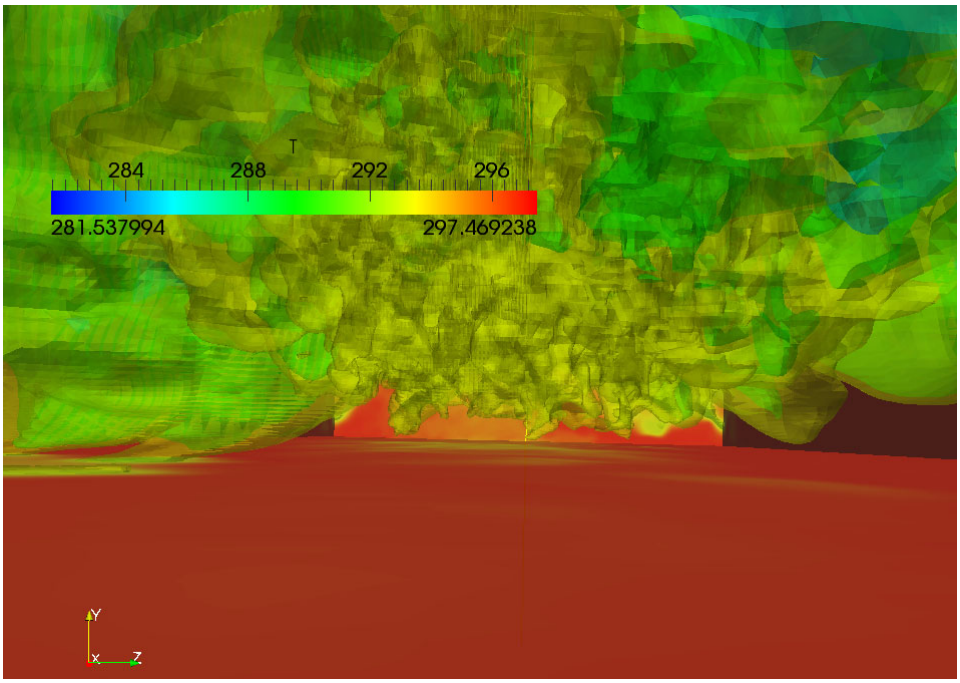

Figure 17.—View from underneath the jet of temperature is-surfaces, showing the re-attachment event.

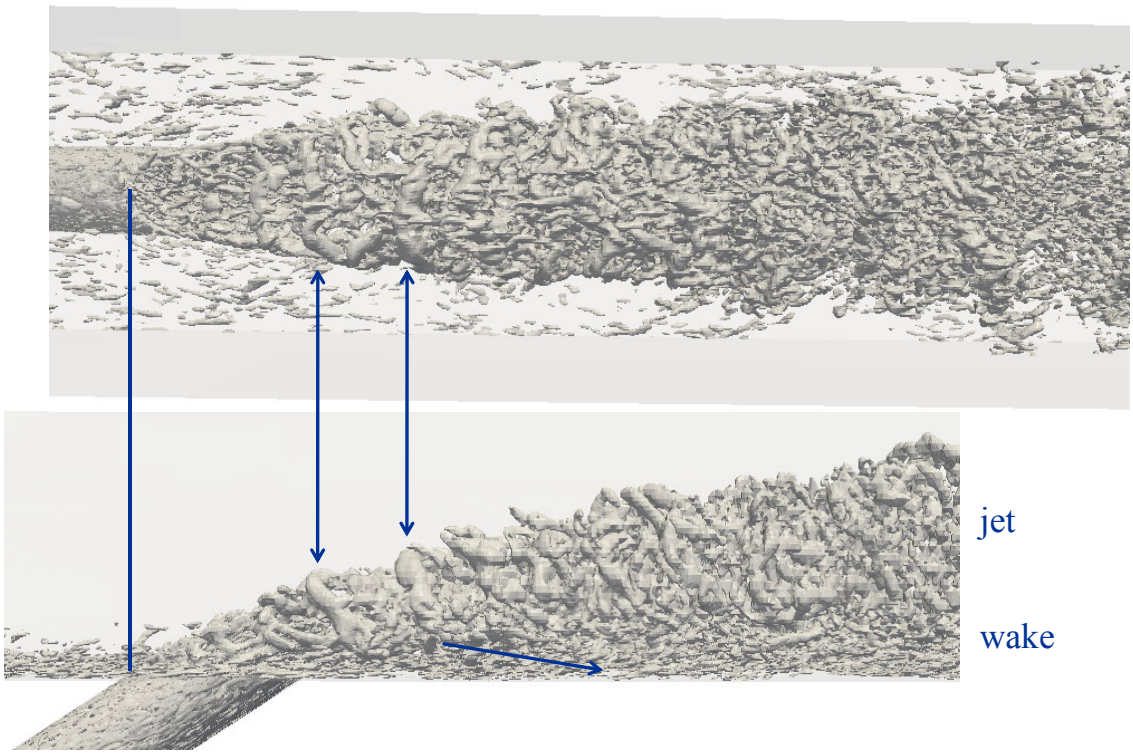

Figure 18.—Iso-surfaces of the lambda-2 criterion for vortex eduction from a top and side view of the jet.

Figure 18 shows iso-surfaces of the lambda-2 criterion for vortex eduction (Jeong and Hussain 1995). The turbulent flow field is obviously very chaotic with a large range of resolved scales. The largest coherent structures are of the most interest, since they are likely most responsible for turbulent mixing and the spreading of the jet. The arrows attempt to link the location of shear layer structures in the two views. The top image, looking down on the jet, reveals spanwise coherent structures riding along the top of the jet. The side image reveals that the large structures are oriented normal to the wall. In fact, the two structures pointed with arrows in Figure 18 show the characteristics of both of these orientations. This evidence reveals an upside-down "U" shape pattern in the large-scale coherent structures. These are linked with the shear layer instability and roll-up seen in the temperature contours. It is interesting to note that these do not occur on the underside of the jet. Instead, smaller coherent structures are found. Indeed, there is a distinct boundary in the presence of these large structures in the upper half of the jet and absence in the lower half (wake region).

Although unable to be visualized in this paper, motion pictures of the structures in Figure 18 reveal a second item of interest. Some structures are pulled, evidently by the motion of the counter-rotating vortex pair, into the wake region along the sides of the jet, where they dissipate on a collision course with the wall. These are in the same region as the unsteady reattachment events noted in the temperature iso-surfaces. Thus, the evidence points to an unsteady separation of large scale shear rollups along the side of the jet from the "U"-shape and subsequent motion toward the wall, creating unsteady re-attachment events of increased adiabatic effectiveness and wall shear stress and higher speed fluid is force in close proximity to the wall.

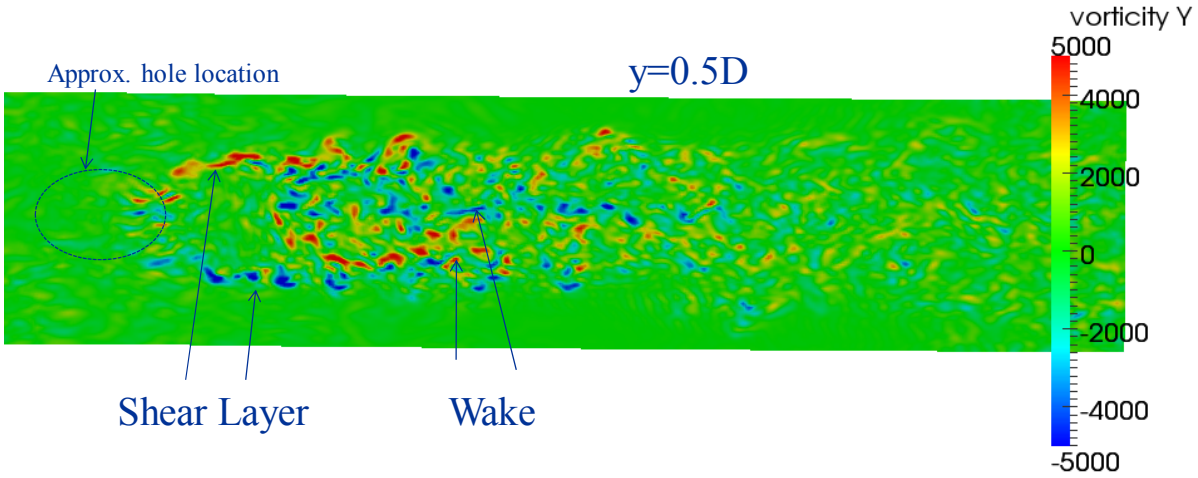

Figure 19.—Y-vorticity at 0.5 diameters above the surface.

A final note from the unsteady structure of the LES flow is to be made concerning the wall normal vorticity, Figure 19. As the jet emerges from the hole, the leading edge (which becomes the upper edge) of the jet is at a higher velocity than the crossflow. This causes vorticity wrapping away from the center of the jet in the shear layer at the top and side of the jet. Meanwhile, wake vortices typically take the form similar to those seen in the wake of a solid cylinder in crossflow. Such wake vorticity is opposite that of the shear layer. Such a pattern is indeed revealed in Figure 19. The figure shows a plane one-half diameter above the surface. In the streamwise direction, the shear layer y-vorticity becomes visible first, as the upper half of the jet passes through the plane. As the lower half passes and the wake reaches into the plane, the vorticity toward the centerline shows a pattern opposite that of the shear layer.

Conclusion

A wall-resolved large-eddy simulation (WR-LES) of a film cooling flow with hig blowing ratio (M = 1.7) was completed to complement the experimental study of El-Gabry (2010). Mean velocity and temperature profiles show good agreement with experimental data, far superior to predictions by the k-ω SST model. Particularly, the spanwise spreading at the sides of the jet and the wall-normal spreading at the upper shear layer of the jet were well-predicted by the LES in the near-hole region. In the region where the jets begin to merge, the LES prediction of spreading does not keep up with the experimental data due to the growing infidelity of the spanwise periodic boundary condition. The region below the jet suffers the most disagreement between the LES predictions and experimental results. It is speculated that the resolution of the grid (size and anisotropy of the implicit filter) was not sufficient for the applicability of a zero-equation sub-grid model in a region of such fine-scale structures near the wall and in the region of high turbulent kinetic energy below the jet. Analysis of the unsteady structures reveal an upside-down "U" shaped tendency around the three free shear layers of the jet. The counter-rotating pair of vortices act in an apparently random manner to pull some of these structures around the side of the jet and toward the surface to create reattachment events on either side of the centerline. Wall-normal wake structures underneath the jet are shown similar to those of Fric and Roshko (1994), with opposite rotation to the shear layer roller vortices on the outer sides of the jet.

Appendix A—Turbulent Boundary Layer Inflow

A common difficulty for LES simulations of engineering wall bounded flows is the difficulty of specifying time-accurate boundary conditions for an approaching turbulent boundary layer. One popular family of techniques is the recycling-rescaling method first introduced by Lund et al. (1994). This method has been updated over the years and many variants have been introduced in open literature, most recently by Jewkes et al. (2011). In these methods, an auxiliary simulation is performed alongside the main simulation in which a plane of the velocity field is extracted and scaled using a blend of inner and outer equilibrium boundary layer scaling. The scaled velocity data is reintroduced at the inlet of the auxiliary simulation and given enough time, a realistic spatially-developing turbulent boundary layer is produced. At this point, velocity planes are extracted from the auxiliary domain and introduced at the inlet of the main simulation.

In the present implementation, the method of Lund et al. (1994) is adopted with some of the modifications of Jewkes et al. (2011). Specifically, the displacement thickness is used instead of the disturbance thickness and the initialization suggestions of Jewkes et al. (2011) are followed. In addition, a modification suggested but not implemented by Lund et al. (1994) is used. This modification is the elimination of the need for the auxiliary solution. Instead, the recycling plane is simply taken from the main simulation itself, scaled, and reintroduced at the inlet. In this way, the need for an auxiliary domain is eliminated. To decrease the cost of the start-up transients in the recycling method, however, a smaller piece upstream of the film cooling hole is extracted from the main grid and the solution is first advanced on this smaller grid until a realistic turbulent boundary layer is produced (Figs. 4 and 6). The velocity field from this smaller simulation is then mapped onto the full grid to initialize the main simulation (Fig. 7). For mathematical details of the method, the reader is referred to the two sources mentioned above.

Appendix B—Turbulent Pipe Inflow

The other flow inlet did not present as much of a challenge because a spatially developing inlet condition was not deemed necessary. The experimental holes were very long (> 15 D) so the goal of the inlet to the holes was to produce fully developed pipe flow. While the experimental holes may not have been perfectly fully developed in 15 diameters (an elbow and t-joint were upstream of the holes), for unsteady simulation purposes, the most reliable and accurate method of reproducing the experiment was the specification of fully developed flow at uniform temperature and adiabatic walls.

The fully developed pipe flow was realized numerically by inserting a recycling plane 5 D downstream of the pipe inlet. No re-scaling was necessary because spatially developing flow was not desired. The velocity profiles were simply recycled to the inlet at each time step. This reliably produced the desired effect with the initialization procedure below. The recycling place was 5 D upstream of the hole exit.

Appendix C—Initialization Methods

Initialization for the upstream boundary layer and coolant pipe inlet recycling sub-domains was accomplished through a procedure similar to that described by Jewkes et al. (2011). The mean flow given by the Spalding law was first applied to the boundary layer thickness and pipe radius. Then random fluctuations were superposed on the mean profile. The random fluctuations were applied in a piece-wise fashion as suggested by Jewkes. Gaussian distributions with standard deviations based on percent of the local velocity were applied and clipped at two standard deviations from the mean. The resulting velocity values were also clipped at the free-stream velocity. The piecewise initialization was similar to those suggested by Jewkes: from 0.05 < y/(delta) < 0.25, standard deviations of 40% for u', 25% for v', and 30% for w', from 0.25 < y/(delta) < 0.5, standard deviations of 20% for u', 12.5% for v', and 15% for w', and from 0.5 < y/(delta) < 1.0, standard deviations of 10% for u', 6.25% for v', and 7.5% for w'. Figure 5 shows the results of this initialization for both sub-domains.

References

Acharya, S., Tyagi, M., and Hoda, A., 2001, "Flow and Heat Transfer Predictions for Film Cooling," Heat Transfer in Gas Turbine Systems, Ann. N.Y. Acad. Sci., Vol. 934, pp. 110–125.

Brittingham, R.A., and Leylek, J.H., 2000, "A Detailed Analysis of Film-Cooling Physics: Part IV – Compound-Angle Injection with Shaped Holes," ASME Journal of Turbomachinery, Vol. 122, pp. 102-112.

Bunker, R.S., 2005, "A Review of Shaped Hole Turbine Film-Cooling Technology," Journal of Heat Transfer, 127, pp. 441-453.

Bunker, R.S., 2001, "A Method for Improving the Cooling Effectiveness of a Gaseous Coolant Stream," US Patent 6,234,755.

Bunker, R.S., 2002, "Film Cooling Effectiveness due to Discrete Holes within a Transverse Trench," Proceedings of the ASME Turbo Expo 2002, Amsterdam, The Netherlands, GT-2002-30178.

El Gabry, L., 2011, "Turbulence and Heat Transfer Measurements in an Inclined Large Scale Film Cooling Array – Part I, Velocity and Turbulence Measurements," ASME Turbo Expo, GT2011-46491.

El Gabry, L., 2011, "Turbulence and Heat Transfer Measurements in an Inclined Large Scale Film Cooling Array – Part II, Temperature and Heat Transfer Measurements," ASME Turbo Expo, GT2011-46498.

Eriksen, V.L., and Goldstein, R.J., 1974, "Heat Transfer and Film Cooling Following Injection Through Inclined Circular Tubes," ASME Journal of Heat Transfer, Vol. 96, pp. 239-245.

Fric, T. F., and Roshko, A., 1994, "Vortical Structure in the Wake of a Transverse Jet," J. Fluid Mech., Vol. 279, pp. 1–47.

Germano, M., Piomelli, U., Moin, P., and Cabot, W.H., 1991, "A Dynamic Subgrid-Scale Eddy Viscosity Model," Phys. Fluids, Vol. 3, No. 7, pp. 1760-1765.

Goldstein, R.J., Eckert, E.R.G., and Ramsey, J.W., 1968, "Film Cooling with Injection Through Holes: Adiabatic Wall Temperatures Downstream of a Circular Hole," ASME Journal of Engineering for Power, Vol. 90, pp. 384-395.

Goldstein, R.J., Eckert, E.R.G., Eriksen, V.L., and Ramsey, J.W., 1970, "Film Cooling Following Injection Through Inclined Circular Tubes," Israel Journal of Technology, Vol. 8, pp. 145-154.

GridPro. Product Development Company, www.gridpro.com

Guo, X., Schröder, W., and Meinke, M, 2006, "Large-eddy Simulations of Film Cooling Flows," Computers and Fluids, Vol. 35, pp. 587–606.

Haven, B.A., and Kurosaka, M., 1997, "Kidney and Anti-Kidney Vortices in Crossflow Jets," J. Fluid Mech., Vol. 352, pp. 27–64.

Haven, B.A., Yamagata, D.K., Kurosaka, M., Yamawaki, S., and Maya, T., 1997, "Anti-Kidney Pair of Vortices in Shaped Holes and Their Influence on Film Cooling Effectiveness," Proceedings of ASME Turbo Expo 1997, Orlando, FL, USA, 97-GT-45.

Hyams, D.G., and Leylek, J.H., 2000, "A Detailed Analysis of Film-Cooling Physics: Part III – Streamwise Injection with Shaped Holes," ASME Journal of Turbomachinery, Vol. 122, pp. 122-132.

Iourokina, I.V., and Lele, S.K., 2006a, "Large Eddy Simulation of Film-Cooling Above the Flat Surface with a Large Plenum and Short Exit Holes," Proceedings of the AIAA Aerospace Sciences Meeting and Exhibit, 2006, Reno, Nevada, USA.

Iourokina, I.V., and Lele, S.K., 2006b, "Large Eddy Simulation of Film Cooling Flow Above a Flat Surface from Inclined Cylindrical Holes," Proceedings of the ASME Joint U.S.-European Fluids Engineering Summer Meeting, 2006, Miami, Florida, USA.

Jeong, J., and Hussain, F., 1995, "On the Identification of a Vortex," J. Fluid Mech., vol. 285, pp. 69-94.

Jewkes, J.W., Chung, Y.M., and Carpenter, P.W., 2011, "Modification to a Turbulent Inflow Generation Method for Boundary-Layer Flows," AIAA J. Technical Note, Vol. 49, No. 1, pp. 247-250.

Johnson, P.L., Nguyen, C.Q., Ho, S.H., and Kapat, J.S., 2010, "Sensitivity Analysis of Domain Considerations for Numerical Simulations of Film Cooling," Proceedings of the 14th ASME International Heat Transfer Conference, IHTC14-23241.

Johnson, P.L., Shyam, V., Hah, C., 2011, "Reynolds-Averaged Navier-Stokes Solutions to Flat Plate Film Cooling Scenarios," NASA/TM—2011-217025.

Kelso, R.M., Lim, T.T., and Perry, A.E., 1996, "An Experimental Study of Round Jets in Cross-flow," Journal of Fluid Mechanics, Vol. 306, pp. 111-144.

Lavrich, P.L., and Chiappetta, L.M., 1990, ''An Investigation of Jet in a Cross Flow for Turbine Film Cooling Applications," United Technologies Research Center, UTRC Report No. 90-04.

Leedom, D.H., and Acharya, S., 2008, "Large Eddy Simulations of Film Cooling Flow Fields From Cylindrical and Shaped Holes," Proceedings of ASME Turbo Expo 2008, Berlin, Germany, GT2008-51009.

Ligrani, P.M., Wigle, J.M., Ciriello, S. and Jackson, S.W., 1994a, "Film-Cooling from Holes with Compound Angle Orientations: Part I – Results Downstream of Two Staggered Rows of Holes with 3d Spanwise Spacing," ASME Journal of Heat Transfer, Vol. 116, pp. 353-362.

Ligrani, P.M., Wigle, J.M., and Jackson, S.W., 1994b, "Film-Cooling from Holes with Compound Angle Orientations: Part II – Results Downstream of a Single Row of Holes with 6d Spanwise Spacing," ASME Journal of Heat Transfer, Vol. 116, pp. 353-362.

Lilly, D.K., 1992, "A Proposed Modification to the Germano Subgrid-Scale Closure Method," Phys. Fluids, Vol. 4, No. 3, pp. 633-635.

Lund, T.S., Wu, X., and Squires, K.D., 1998, "Generation of Turbulent Inflow Data for Spatially Developing Boundary Layer Simulations," J. Comp. Phys., Vol. 140, pp. 233-258.

McGovern, K.T., and Leylek, J.H., 2000, "A Detailed Analysis of Film-Cooling Physics: Part II – Compound-Angle Injection with Cylindrical Holes," ASME Journal of Turbomachinery, Vol. 122, pp. 113-121.

OpenFOAM®, www.openfoam.com

Peet, Y.V., and Lele, S.K., 2008, "Near Field of Film Cooling Jet Issued Into a Flat Plate Boundary Layer: LES Study," GT2008-50420, Proceedings of ASME Turbo Expo 2008, Berlin, Germany.

Renze, P., Schroder, W., Meinke, M., 2008a, "Large-Eddy Simulation of Film Cooling Flows at Density Gradients," International Journal of Heat and Fluid Flow, Vol. 29, pp. 18-34.

Renze, P., Schroder, W., Meinke, M., 2008b, "Large-Eddy Simulation of Film Cooling Flows with Variable Density Jets," Flow Turbulence and Combustion, Vol. 80, 119-132.

Renze, P., Schroder, W., and Meinke, M., 2008c, "Large-Eddy Simulation of Film Cooling Flow Ejected in a Shallow Cavity," Proceedings of the ASME Turbo Expo 2008, Berlin, Germany, GT2008-50120.

Renze, P., Schroder, W., and Meinke, M., 2009, "Large-Eddy Simulation of Interacting Film Cooling Jets," Proceedings of the ASME Turbo Expo 2009, Orlando, Florida, USA, BT2009-59164.

Schmidt, D.L., Sen, B., and Bogard, D.G., 1996, "Film Cooling with Compound Angle Holes – Adiabatic Effectiveness," ASME Journal of Turbomachinery, Vol. 118, 807-813.

Sen, B., Schmidt, D.L., and Bogard, D.G., 1996, "Film Cooling with Compound Angle Holes – Heat Transfer," ASME Journal of Turbomachinery, Vol. 118, pp. 800-806.

Sinha, A.K., Bogard, D.G., and Crawford, M.E., 1991, "Film-Cooling Effectiveness Downstream of a Single Row of Holes with Variable Density Ratio," ASME Journal of Turbomachinery, Vol. 113, pp. 442-449.

Tyagi, M., and Acharya, S., 2003, "Large Eddy Simulation of Film Cooling Flow from an Inclined Cylindrical Jet," J Fluid Mech, Vol. 125, pp 734-742.

Walters, D.K., and Leylek, J.H., 2000, "A Detailed Analysis of Film-Cooling Physics: Part I – Streamwise Injection with Cylindrical Holes," ASME Journal of Turbomachinery, Vol. 122, pp. 102-112.

REPORT DOCUMENTATION PAGE	Form Approved OMB No. 0704-0188

1. REPORT DATE *(DD-MM-YYYY)*	2. REPORT TYPE	3. DATES COVERED *(From - To)*
01-08-2012	Technical Memorandum	

4. TITLE AND SUBTITLE
Large Eddy Simulation of a Film Cooling Flow Injected From an Inclined Discrete Cylindrical Hole Into a Crossflow With Zero-Pressure Gradient Turbulent Boundary Layer

5a. CONTRACT NUMBER
NNC097A01C

5b. GRANT NUMBER

5c. PROGRAM ELEMENT NUMBER

6. AUTHOR(S)
Johnson, Perry, L.; Shyam, Vikram

5d. PROJECT NUMBER

5e. TASK NUMBER

5f. WORK UNIT NUMBER
WBS 561581.02.08.03.21.14.03

7. PERFORMING ORGANIZATION NAME(S) AND ADDRESS(ES)
National Aeronautics and Space Administration
John H. Glenn Research Center at Lewis Field
Cleveland, Ohio 44135-3191

8. PERFORMING ORGANIZATION REPORT NUMBER
E-18382

9. SPONSORING/MONITORING AGENCY NAME(S) AND ADDRESS(ES)
National Aeronautics and Space Administration
Washington, DC 20546-0001

10. SPONSORING/MONITOR'S ACRONYM(S)
NASA

11. SPONSORING/MONITORING REPORT NUMBER
NASA/TM-2012-217695

12. DISTRIBUTION/AVAILABILITY STATEMENT
Unclassified-Unlimited
Subject Categories: 02, 34, and 61
Available electronically at http://www.sti.nasa.gov
This publication is available from the NASA Center for AeroSpace Information, 443-757-5802

13. SUPPLEMENTARY NOTES

14. ABSTRACT
A Large Eddy Simulation (LES) is performed of a high blowing ratio (M = 1.7) film cooling flow with density ratio of unity. Mean results are compared with experimental data to show the degree of fidelity achieved in the simulation. While the trends in the LES prediction are a noticeable improvement over Reynolds-Averaged Navier-Stokes (RANS) predictions, there is still a lack a spreading on the underside of the lifted jet. This is likely due to the inability of the LES to capture the full range of influential eddies on the underside of the jet due to their smaller structure. The unsteady structures in the turbulent coolant jet are also explored and related to turbulent mixing characteristics.

15. SUBJECT TERMS
Film cooling; Turbulence model; Heat transfer

16. SECURITY CLASSIFICATION OF:			17. LIMITATION OF ABSTRACT	18. NUMBER OF PAGES	19a. NAME OF RESPONSIBLE PERSON
a. REPORT	b. ABSTRACT	c. THIS PAGE			STI Help Desk (email:help@sti.nasa.gov)
U	U	U	UU	27	19b. TELEPHONE NUMBER *(include area code)* 443-757-5802